research article

An image fusion system for estimating the therapeutic effects of radiofrequency ablation on hepatocellular carcinoma

Nobuyuki Toshikuni, Yasuhiro Matsue, Kazuaki Ozaki, Kaho Yamada, Nobuhiko Hayashi, Mutsumi Tsuchishima, Mikihiro Tsutsumi

Department of Hepatology, Kanazawa Medical University, Uchinada, Ishikawa, Japan

Radiol Oncol 2017; 51(3): 263-269.

Received 3 December 2016
Accepted 29 June 2017

Correspondence to: Nobuyuki Toshikuni, M.D., Ph.D., Department of Hepatology, Kanazawa Medical University, 1-1 Daigaku, Uchinada-machi, Kahoku, Ishikawa 920-0293, Japan. Phone: +81 76 286 2211; Fax: +81 76 286 0892; E-mail: n.toshikuni@gmail.com

Disclosure: The authors declare no potential conflicts of interest.

Background. During ultrasound-guided radiofrequency ablation (RFA) of hepatocellular carcinoma (HCC), high echoic areas due to RFA-induced microbubbles can help calculate the extent of ablation. However, these areas also decrease visualization of target tumors, making it difficult to assess whether they completely cover the tumors. To estimate the effects of RFA more precisely, we used an image fusion system (IFS).

Patients and methods. We enrolled patients with a single HCC who received RFA with or without the IFS. In the IFS group, we drew a spherical marker along the contour of a target tumor on reference images immediately after administering RFA so that the synchronized spherical marker represented the contour of the target tumor on real-time ultrasound images. When the high echoic area completely covered the marker, we considered the ablation to be complete. We compared outcomes between the IFS and control groups.

Results. We enrolled 25 patients and 20 controls, and the baseline characteristics were similar between the two groups. The complete ablation rates during the first RFA session were significantly higher in the IFS group compared with those in the control group (88.0% *vs*. 60.0%, $P = 0.041$). The number of RFA sessions was significantly smaller in the IFS group compared with that in the control group (1.1 ± 0.3 *vs*. 1.5 ± 0.7, $P = 0.016$).

Conclusions. The study suggested that the IFS enables a more precise estimation of the effects of RFA on HCC, contributing to enhanced treatment efficacy and minimized patient burden.

Key words: image fusion; hepatocellular carcinoma; radiofrequency ablation

Introduction

Radiofrequency ablation (RFA) is an established curative, non-surgical method for treating small hepatocellular carcinoma (HCC) [1], and ultrasound (US) is the most widely used imaging modality for RFA procedures because of its convenience and simplicity. During US-guided RFA, a high echoic area due to RFA-induced microbubbles emerges and then enables calculation of the ablation extent.[2,3] However, the high echoic area also decreases visualization of target tumors, making it difficult to assess whether the area completely covers the tumor. A method that can overcome this issue would increase the efficiency of RFA and thus decrease the number of treatments required and prevent further distress to patients due to re-treatment.

Recent advances in imaging technologies have enabled image fusion among stored computed tomography (CT), magnetic resonance imaging (MRI), US images and real-time US images on the same US monitor, called real-time image fusion (RTIF).[4,5] Numerous studies on RFA for HCC have shown that RTIF can help target tumors that are inconspicuous on US but detectable on CT and/or MRI. These studies reported that tumor targeting was successful (53–100%) for detecting several inconspicuous tumor cases.[6-12]

In this study, we hypothesized that tumor marking with an image fusion system (IFS) may be useful for assessing the positional relationship between target tumors and high echoic areas during RFA and could thereby more precisely estimate the effects of RFA on HCC. The primary aim of this study was to compare complete ablation rates in the first RFA session between patients receiving RFA with or without use of this method. The secondary aim was to compare the number of RF electrode insertions, number of RFA sessions, and local recurrence rates among patients.

Patients and methods

Patients

We performed a historically controlled study by prospectively enrolling patients with a single HCC who received RFA with the IFS between April 2012 and May 2016. HCC patients who received RFA without the method between October 2011 and March 2012 served as controls. We diagnosed HCC based on the results of contrast enhanced US (CEUS), dynamic CT, and dynamic MRI in combination with serum tumor markers.[13] For CEUS, we used perfluorobutane (Sonazoid; GE Healthcare, Amersham Place, UK) as an US contrast agent.[14,15] We selected RFA as a curative treatment for HCC according to the Clinical Practice Guidelines for Hepatocellular Carcinoma (the J-HCC guidelines), which were the first evidence-based clinical practice guidelines for the treatment of HCC in Japan.[16]

This study protocol was approved by the Ethical Committee of Kanazawa Medical University (approval number 236). We obtained informed consent from all patients and performed all procedures according to the guidelines of the Helsinki Declaration.

RFA procedure

Three experienced operators (N.T., Y.M., and N.H.) performed RFA using a cooled-tip RFA system (Covidien, Mansfield, MA, USA) in which a 480-kHz monopolar RF generator was connected to a 17-gauge, internally cooled-tip electrode with a 2- or 3-cm tip. After administration of a sedative agent, an operator percutaneously inserted the electrode into the target tumor under US guidance using an US machine (HI VISION Preirus, Hitachi Ltd., Tokyo, Japan) and a 3.5-MHz microconvex probe (EUP-B512, Hitachi Ltd.). In the event an inconspicuous tumor was identified upon US, we performed RFA under CEUS guidance.[17] After the operator appropriately placed the RF electrode, assistants slowly increased the generator output to 80-120 watts and maintained this output for up to 12 minutes. If the tumor was located under the diaphragm (segment VII or VIII according to the Couinaud classification) or near the liver surface, we performed RFA using artificial ascites and/or pleural effusion to facilitate US guidance and avoid damaging the diaphragm or the parietal peritoneum.[18] We performed RFA following transcatheter arterial chemoembolization for tumors approximately 25-mm or more in size.[19]

Estimation of the RFA effects with the IFS

To estimate the effects of RFA more precisely, we used Real-time Virtual Sonography™ (Hitachi Ltd.), which is an RTIF system consisting of an US machine (HI VISION Preirus, Hitachi Ltd.), a 3.5-MHz microconvex probe (EUP-B512, Hitachi Ltd.) equipped with a magnetic sensor, a transmitter to generate a magnetic field, and a magnetic position detection unit.[5] To create reference images for RTIF, we obtained and stored CEUS and dynamic CT and/or MRI images acquired prior to treatment as three-dimensional volume data in the US machine. We selected an image series that clearly depicted the target tumor and landmark structures of the hepatic parenchyma, such as intrahepatic vessels. To obtain the CEUS volume data, we performed a sweep scan with the 3.5-MHz microconvex probe after injecting Sonazoid™ (GE Healthcare) to ensure the scan covered both the target tumor and the surrounding hepatic parenchyma and then stored the scanned data.[15]

During RFA, a high echoic area due to RFA-induced microbubbles emerged around the position of the RF electrode tip and decreased visualization of the target tumor. Moreover, an acoustic shadow occurred behind the high echoic area, which obscured the posterior boundary line between the area and the hepatic parenchyma; however, approximately 5 minutes after RFA, this acoustic shadow had almost disappeared.

Immediately after RFA, operators retrieved the stored volume data and created reference images or planar images showing the target tumor and the surrounding hepatic parenchyma prior to treatment. We selected the data set that most clearly depicted the target tumor and landmark structures of the hepatic parenchyma. Using Real-time Virtual Sonography™ (Hitachi Ltd.), operators performed

an image fusion between the reference images and real-time US images as follows: As the first step of image fusion, operators matched the tip of the xiphoid process on reference images to the structure on real-time US images and coregistered the reference images and the real-time US images in the sagittal plane of the left hepatic lobe. Next, while scanning on or around the insertion site, operators repeated the coregistration until they achieved correct image fusion. During coregistration, operators asked patients to hold their breath. The US machine had a marking function that automatically displayed synchronized straight and spherical markers on reference images and real-time US images, respectively. Operators drew straight markers along intrahepatic vessels and ensured correct image fusion. They also drew a spherical marker along the target tumor contour on the reference images to show its maximum diameter. The size of the spherical marker was designed to change inversely with the distance between the center of the marker and the scanning section. Thus, the synchronized spherical marker was drawn on real-time US images in all directions, indicating the exact position of the tumor contour that had been poorly visualized immediately after RFA (Figure 1).

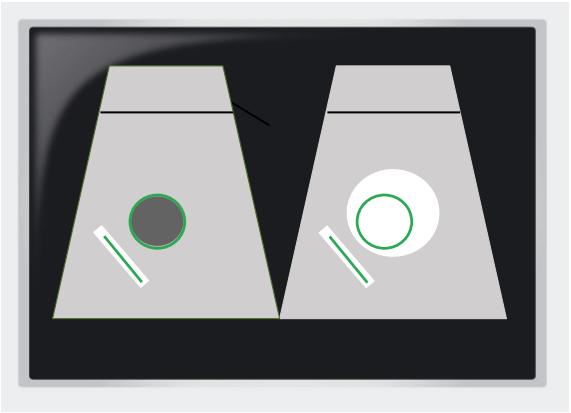

FIGURE 1. Schema of our IFS. An US monitor shows a reference image (left) and a real-time US image (right) immediately after RFA. Two synchronized straight markers depicted in identical positions in the same intrahepatic vessels ensure correct image fusion. On the reference image, a spherical marker (unfilled green circle) was drawn along the contour of a target tumor (filled black circle). On the real-time US image, a high echoic area (filled white circle) due to RFA-induced microbubbles completely covers the synchronized spherical marker, indicating the exact position of the tumor contour, suggesting potential complete ablation.

IFS = image fusion system; RFA = radiofrequency ablation; US = ultrasound

After performing image fusion and tumor marking, operators scanned the ablation area and assessed the positional relationship between the high echoic area and the spherical marker. Once the high echoic area surrounded the spherical marker in all directions with a margin of several millimeters, we considered the ablation to be complete. If the target tumor was located adjacent to vessels or near the liver surface, a partially insufficient margin at the sites was acceptable. If the ablation was deemed incomplete, operators performed additional RF electrode insertions.

Assessment of the RFA effects

We performed dynamic CT or MRI scans 1 or 2 days after RFA. Experienced radiologists blinded to whether the patients received RFA with or without the IFS assessed the RFA effects by viewing images acquired pre-treatment and post-treatment side by side. The complete ablation criteria included that an RFA-induced avascular area surrounded the original target tumor with a margin of several millimeters.[20] When tumors were located adjacent to vessels or near the liver surface, partially insufficient margins at the sites were acceptable. After the radiologists assessed the RFA effects, we evaluated the assessment results. If difficulty was encountered when assessing treatment completeness, we discussed the treatment effects with the radiologists. If the effects did not meet the above criteria, we performed an additional RFA.

Surveillance after RFA

After completing RFA, patients were subjected to imaging and laboratory examinations every 3–6 months. When recurrent HCCs were detected, the patients received appropriate treatment according to the J-HCC guidelines.[16] HCCs detected adjacent to ablated tumors were considered local recurrence tumors.

Statistical analysis

Data are expressed as the mean ± standard deviation. We used Student's t-test and the Fisher's exact probability test to compare continuous variables and categorical variables, respectively. We used the Kaplan-Meier method to calculate local recurrence rates and performed log-rank tests to evaluate the rate differences. We considered a P-value < 0.05 as significant. We performed statistical analysis using

STATA version 13.1 software (StataCorp, College Station, TX, USA).

Results

We enrolled 25 patients who received RFA in combination with the IFS, and 20 patients who received conventional RFA as controls. The baseline characteristics were similar between the two patient groups (Table 1). We were able to use the image fusion method for all 25 patients, and retrieving the stored data, performing image fusion and tumor marking, and estimating the effects of RFA took approximately 10 minutes. The complete ablation rate during the first RFA session was significantly higher in the IFS group than in the control group (88% [22/25] vs. 60% [12/20], $P = 0.041$). Incomplete ablation during the first RFA session in the IFS group was due to an insufficient margin (n = 3), while incomplete ablation during the first RFA session in the control group was due to an unablated residual tumor (n = 4) and an insufficient margin (n = 4). The number of RFA sessions was significantly smaller in the IFS group than in the control group (1.1 ± 0.3 [1, n = 22; 2, n = 3] vs. 1.5 ± 0.7 [1, n = 12; 2, n = 6; 3, n = 2], $P = 0.016$), and the total number of RF electrode insertions was not significantly different between the two groups (2.0 ± 0.9 [1, n = 9; 2, n = 9; 3, n = 6; 4, n = 1] vs. 2.3 ± 1.5 [1, n = 7; 2, n = 5; 3, n = 6; 4, n = 1; 7, n = 1], $P = 0.18$). There were no severe RFA-related complications in any of the patients. In this study, we presented two HCC cases in which we performed RFA using this method (Figures 2 and 3). In case 2, we considered the ablation incomplete after the first RF electrode insertion during the first RFA session. Owing to the positional information gained from the image fusion method, we could easily identify portions of the tumor requiring additional RF electrode in-

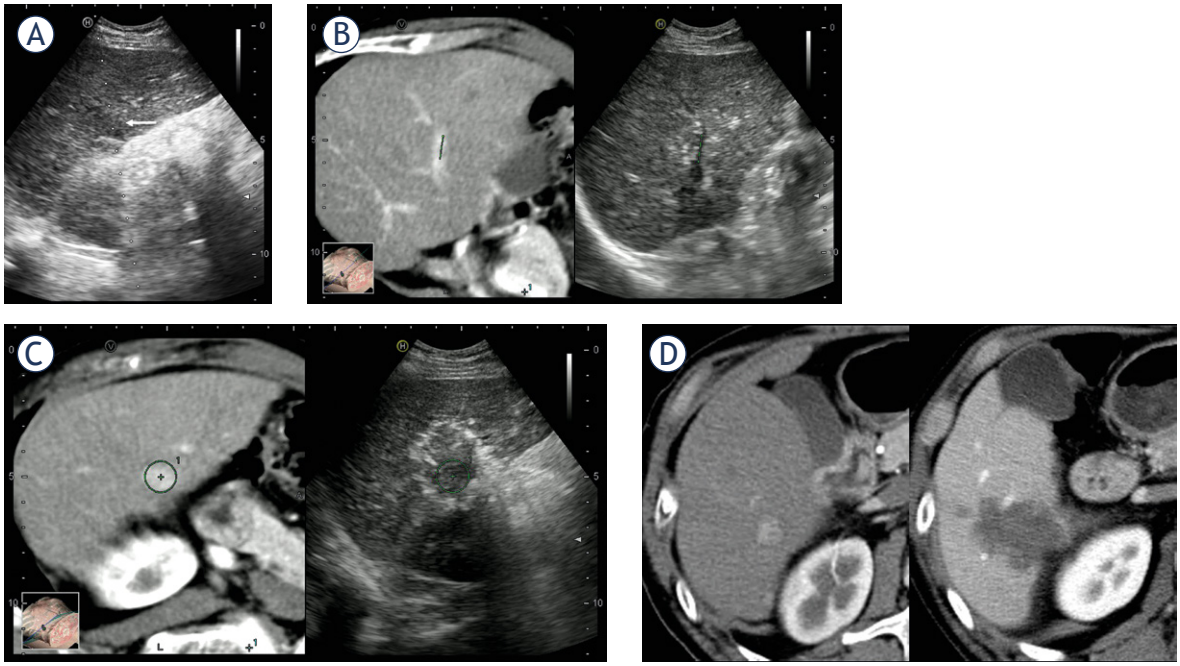

FIGURE 2. *Case 1.* A 67-year-old male patient had a 15-mm HCC in segment VI. **(A)** The HCC is depicted as a low echoic tumor (white arrow) on US. A dot-line represents a puncture line for RFA. **(B)** A reference CT image (left) and a real-time US image (right) immediately after the first RF electrode insertion in the first RFA session. In this case, reference images were created by retrieving pre-treatment arterial phase images from a dynamic CT. Two synchronized straight markers depicted at the same positions in the same portal vein branches ensured correct image fusion. **(C)** Another reference CT image depicting the tumor (right) and the corresponding real-time US image (left). On the reference image, a spherical marker was drawn along the tumor contour. On the real-time US image, the tumor is almost invisible because of a high echoic area due to RFA-induced microbubbles. However, the synchronized spherical marker indicates the exact position of the tumor contour. The high echoic area completely covers the synchronized spherical marker, thus suggesting the potential complete ablation. **(D)** Pre-treatment (left) and post-treatment (right) dynamic CT images. The pre-treatment arterial phase image depicts a hypervascular tumor, while the post-treatment portal phase image depicts an RFA-induced avascular area larger than the original tumor. These findings are suggestive of the achievement of complete ablation after the first RFA session.

CT = computed tomography; HCC = hepatocellular carcinoma; RFA = radiofrequency ablation; US = ultrasound

TABLE 1. Baseline characteristics of patients

	IFS group (n = 25)	Control group (n = 20)	*P*-value *
Age (years)	73 ± 8 ¤	74 ± 9 ¤	0.39
Sex, male/female	14/11	8/12	0.37
Etiology, viral/non-viral	15/10	17/3	0.10
Child-Pugh grade, A/B	22/3	16/4	0.68
Occurrence, new/recurrent	23/2	18/2	1.00
Tumor size (mm)	19 ± 6 ¤	19 ± 8 ¤	0.42
Tumor location, L/M/A/P	2/4/11/8	0/2/11/7	0.53
Tumor vascularity, hypo/hyper	3/22	1/19	0.62
Electrode tip, 2 cm/3 cm	9/16	2/18	0.08
CEUS guidance for RFA, no/yes	22/3	18/2	1.00
Artificial ascites and/or pleural effusion, no/yes	12/13	8/12	0.76
Combined with TACE, no/yes	21/4	18/2	0.68

IFS = image fusion system; L = lateral segment; M = medial segment; A = anterior segment; P = posterior segment; CEUS = contrast enhanced ultrasound; RFA = radiofrequency ablation; TACE = transcatheter arterial chemoembolization. ¤ Data are expressed as the mean ± standard deviation. * Student's t-tests and Fisher's exact probability tests were used for continuous variables and categorical variables, respectively.

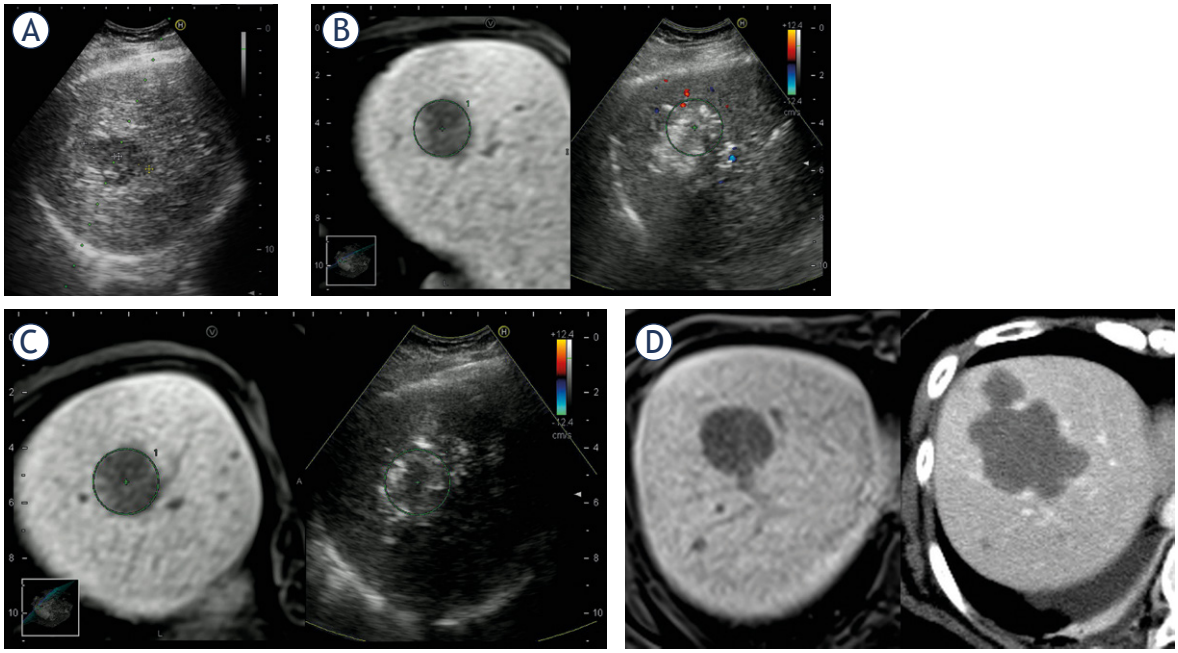

FIGURE 3. *Case 2.* A 66-year-old female patient had a 28-mm HCC in segment VIII. **(A)** The HCC is depicted as a low echoic tumor on US. A dot-line represents a puncture line for RFA. **(B)** A reference MRI image (left) and a real-time US image (right) immediately after the first RF electrode insertion in the first RFA session. In this case, reference images were created by retrieving pre-treatment hepatobiliary phase images of Gd-EOB-DTPA-enhanced MRI. On the reference image, a spherical marker was drawn along the tumor contour. Although the tumor is almost invisible on the real-time US image because of a high echoic area due to RFA-induced microbubbles, the synchronized spherical marker indicates the exact position of the tumor contour. The positional relationship between the high echoic area and the synchronized spherical marker suggests incomplete ablation. **(C)** A reference MRI image (left) and a real-time US image (right) immediately after the fourth RF electrode insertion in the first RFA session. The extent of the high echoic area due to RFA-induced microbubbles is larger than that after the first RF electrode insertion. The positional relationship between the high echoic area and the synchronized spherical marker suggests potential complete ablation. **(D)** A pre-treatment MRI image (left) and a post-treatment dynamic CT image (right). The pre-treatment hepatobiliary image depicts a hypointense tumor, while the post-treatment portal phase image depicts an RFA-induced avascular area larger than the original tumor. These findings are suggestive of the achievement of complete ablation after the first RFA session.

CT = computed tomography; Gd-EOB-DTPA = gadolinium-ethoxybenzyl-diethylenetriamine pentaacetic acid; HCC = hepatocellular carcinoma; MRI = magnetic resonance imaging; RFA = radiofrequency ablation; US = ultrasound

sertions. Thus, we performed additional ablations and completely ablated the tumor in a single RFA session.

During a mean follow-up period of 27 months (IFS group, 21 months [range 1–36 months]; control group, 34 months [range 2–63 months]), the cumulative local recurrence rates at 36 months were 8.3% in the IFS group and 12.6% in the control group, which were not significantly different ($P = 0.98$).

Discussion

The present study demonstrated that using an IFS permits precise estimation of the effects of RFA on HCC and thus aids in deciding whether to perform additional RF electrode insertions in an RFA session and identifying tumor portions requiring additional RF electrode insertions. In most cases, use of our method resulted in complete ablation in a single RFA session. Minimizing the number of treatment sessions would reduce patient distress, the risk of treatment complications and treatment costs. In an earlier study, Hiraoka *et al.* succeeded in precisely estimating the effects of RFA on HCC via an RTIF method using a workstation.[21] In accordance with the results of our study, Hiraoka *et al*. demonstrated that RFA using their method decreased the number of treatment sessions required. Because of recent advances in imaging modalities, clinicians can now perform RTIF on a single US machine without a workstation, which may facilitate routine use of this IFS in RFA of HCC.

Our IFS is advantageous for performing RFA for HCC. A major limitation of RFA is poor conspicuity on US. Isoechoic tumors, small tumors, and surrounding coarse, nodular liver parenchyma are reported causes of poor conspicuity.[5] Conventional RTIF has overcome this issue, leading to successful RFA for tumors undetectable via US.[6–12] High echoic areas due to RFA-induced microbubbles are another cause of poor target tumor conspicuity, which makes precise estimation of therapeutic effects difficult. Using a marking function in our IFS provides a solution to poor conspicuity during RFA, as this technology allows operators to recognize the exact position of poorly visualized target tumors in high echoic areas, thus leading to precise estimation of the effects of RFA.

We previously reported the utility of the IFS in assessing the effects of RFA on HCC.[15] In a previous study, we discussed the possibility of reducing the number of dynamic CT scans when assessing the effects of RFA, and several studies have presented similar results to this effect.[22] The results of past and present studies regarding this method will enable US to be used more frequently for diagnosing HCC, performing RFA, and assessing RFA effects, especially when US volume data can be the reference image source for image fusion. In a recent study, Minami *et al.* reported that an image fusion method using US reference images could allow precise estimation of the effects of RFA on liver metastases.[23] Hence, the IFS may potentially increase the efficiency of using RFA for HCC.

Our method does, however, have several limitations. First, we used spherical markers so that the markers indicated the exact positions of tumor contours that are poorly visualized on real-time US images immediately after RFA. However, tumor contours are not perfectly spherical, and discrepancy between the markers and actual tumor contours may occasionally make estimating ablation margins difficult. Indeed, there were three cases of incomplete ablation after the first RFA session in the IFS group. Second, correct image fusion may be difficult for patients who cannot hold their breath for a certain amount of time (approximately 10 seconds). Third, patients with pacemakers are not eligible for RFA with RTIF because this method uses a magnetic field. Fourth, only high-end US machines currently incorporate RTIF systems, and additional time would be required for such systems to be readily available in clinical practice.

In conclusion, our study suggested that the present method could enhance the efficiency of RFA for HCC and minimize patient burden. Further studies with a larger number of patients would confirm the benefits of RFA with the IFS for the treatment of HCC.

Acknowledgements

We are most grateful to Mr. Makoto Mishita and Ms. Eriko Matsuoka, Hitachi Ltd., for their excellent technical support.

References

1. Tiong L, Maddern GJ. Systematic review and meta-analysis of survival and disease recurrence after radiofrequency ablation for hepatocellular carcinoma. *Br J Surg* 2011; **98:** 1210-24. doi:10.1002/bjs.7669

2. Nouso K, Shiraga K, Uematsu S, Okamoto R, Harada R, Takayama S, et al. Prediction of the ablated area by the spread of microbubbles during radiofrequency ablation of hepatocellular carcinoma. *Liver Int* 2005; **25:** 967-72. doi:10.1111/j.1478-3231.2005.01145.x

3. Koda M, Mandai M, Matono T, Sugihara T, Nagahara T, Ueki M, et al. Assessment of the ablated area after radiofrequency ablation by the spread of bubbles: comparison with virtual sonography with magnetic navigation. *Hepatogastroenterology* 2011; **58:** 1638-42. doi:10.5754/hge08641

4. Minami Y, Kudo M. Ultrasound fusion imaging of hepatocellular carcinoma: a review of current evidence. *Dig Dis* 2014; **32:** 690-5. doi:10.1159/000368001

5. Toshikuni N, Tsutsumi M, Takuma Y, Arisawa T. Real-time image fusion for successful percutaneous radiofrequency ablation of hepatocellular carcinoma. *J Ultrasound Med* 2014; **33:** 2005-10. doi:10.7863/ultra.33.11.2005

6. Kawasoe H, Eguchi Y, Mizuta T, Yasutake T, Ozaki I, Shimonishi T, et al. Radiofrequency ablation with the real-time virtual sonography system for treating hepatocellular carcinoma difficult to detect by ultrasonography. *J Clin Biochem Nutr* 2007; **40:** 66-72. doi:10.3164/jcbn.40.66

7. Kitada T, Murakami T, Kuzushita N, Minamitani K, Nakajo K, Osuga K, et al. Effectiveness of real-time virtual sonography-guided radiofrequency ablation treatment for patients with hepatocellular carcinomas. *Hepatol Res* 2008; **38:** 565-71. doi:10.1111/j.1872-034X.2007.00308.x

8. Minami Y, Chung H, Kudo M, Kitai S, Takahashi S, Inoue T, et al. Radiofrequency ablation of hepatocellular carcinoma: value of virtual CT sonography with magnetic navigation. *AJR Am J Roentgenol* 2008; **190:** W335-41. doi:10.2214/ajr.07.3092

9. Nakai M, Sato M, Sahara S, Takasaka I, Kawai N, Minamiguchi H, et al. Radiofrequency ablation assisted by real-time virtual sonography and CT for hepatocellular carcinoma undetectable by conventional sonography. *Cardiovasc Intervent Radiol* 2009; **32:** 62-9. doi:10.1007/s00270-008-9462-x

10. Lee MW, Rhim H, Cha DI, Kim YJ, Choi D, Kim YS, et al. Percutaneous radiofrequency ablation of hepatocellular carcinoma: fusion imaging guidance for management of lesions with poor conspicuity at conventional sonography. *AJR Am J Roentgenol* 2012; **198:** 1438-44. doi:10.2214/ajr.11.7568

11. Song KD, Lee MW, Rhim H, Cha DI, Chong Y, Lim HK. Fusion imaging-guided radiofrequency ablation for hepatocellular carcinomas not visible on conventional ultrasound. *AJR Am J Roentgenol* 2013; **201:** 1141-7. doi:10.2214/ajr.13.10532

12. Ahn SJ, Lee JM, Lee DH, Lee SM, Yoon JH, Kim YJ, et al. Real-time US-CT/MR Fusion Imaging for Percutaneous Radiofrequency Ablation of Hepatocellular Carcinoma. *J Hepatol* 2016. doi:10.1016/j.jhep.2016.09.003

13. Bruix J, Sherman M, Practice Guidelines Committee, American Association for the Study of Liver Diseases. Management of hepatocellular carcinoma. *Hepatology* 2005; **42:** 1208-36. doi:10.1002/hep.20933

14. Hatanaka K, Kudo M, Minami Y, Ueda T, Tatsumi C, Kitai S, et al. Differential diagnosis of hepatic tumors: value of contrast-enhanced harmonic sonography using the newly developed contrast agent, Sonazoid. *Intervirology* 2008; **51(Suppl 1):** 61-9. doi:10.1159/000122600

15. Toshikuni N, Shiroeda H, Ozaki K, Matsue Y, Minato T, Nomura T, et al. Advanced ultrasonography technologies to assess the effects of radiofrequency ablation on hepatocellular carcinoma. *Radiol Oncol* 2013; **47:** 224-9. doi:10.2478/raon-2013-0033

16. Kudo M, Izumi N, Kokudo N, Matsui O, Sakamoto M, Nakashima O, et al. Management of hepatocellular carcinoma in Japan: Consensus-Based Clinical Practice Guidelines proposed by the Japan Society of Hepatology (JSH) 2010 updated version. *Dig Dis* 2011; **29:** 339-64. doi:10.1159/000327577

17. Minami T, Minami Y, Chishina H, Arizumi T, Takita M, Kitai S, et al. Combination guidance of contrast-enhanced US and fusion imaging in radiofrequency ablation for hepatocellular carcinoma with poor conspicuity on contrast-enhanced US/fusion imaging. *Oncology* 2014; **87(Suppl 1):** 55-62. doi:10.1159/000368146

18. Uehara T, Hirooka M, Ishida K, Hiraoka A, Kumagi T, Kisaka Y, et al. Percutaneous ultrasound-guided radiofrequency ablation of hepatocellular carcinoma with artificially induced pleural effusion and ascites. *J Gastroenterol* 2007; **42:** 306-11. doi:10.1007/s00535-006-1949-0

19. Takuma Y, Takabatake H, Morimoto Y, Toshikuni N, Kayahara T, Makino Y, et al. Comparison of combined transcatheter arterial chemoembolization and radiofrequency ablation with surgical resection by using propensity score matching in patients with hepatocellular carcinoma within Milan criteria. *Radiology* 2013; **269:** 927-37. doi:10.1148/radiol.13130387

20. Kim YS, Lee WJ, Rhim H, Lim HK, Choi D, Lee JY. The minimal ablative margin of radiofrequency ablation of hepatocellular carcinoma (> 2 and < 5 cm) needed to prevent local tumor progression: 3D quantitative assessment using CT image fusion. *AJR Am J Roentgenol* 2010; **195:** 758-65. doi:10.2214/AJR.09.2954

21. Hiraoka A, Hirooka M, Koizumi Y, Hidaka S, Uehara T, Ichikawa S, et al. Modified technique for determining therapeutic response to radiofrequency ablation therapy for hepatocellular carcinoma using US-volume system. *Oncol Rep* 2010; **23:** 493-7.

22. Numata K, Fukuda H, Morimoto M, Kondo M, Nozaki A, Oshima T, et al. Use of fusion imaging combining contrast-enhanced ultrasonography with a perflubutane-based contrast agent and contrast-enhanced computed tomography for the evaluation of percutaneous radiofrequency ablation of hypervascular hepatocellular carcinoma. *Eur J Radiol* 2012; **81:** 2746-53. doi:10.1016/j.ejrad.2011.11.052

23. Minami Y, Minami T, Chishina H, Kono M, Arizumi T, Takita M, et al. US-US Fusion Imaging in Radiofrequency Ablation for Liver Metastases. *Dig Dis* 2016; **34:** 687-91. doi:10.1159/000448857